GEOPHYSICAL RESEARCH LETTERS, VOL. 22, NO. 23, PAGES 3151-3154, DECEMBER 1, 1995

Comparison of broadband and short-period seismic waveform stacks: Implications for upper-mantle discontinuity structure

Jeroen Ritsema, Michael Hagerty and Thorne Lay

Institute of Tectonics, University of California, Santa Cruz

Abstract. Stacks of short-period and broadband seismic waveforms from four deep (h > 550 km) earthquakes in South America recorded in California exhibit small amplitude signals between the direct P and surface-reflected pP phases. The anomalous and variable slownesses of these signals in short-period stacks, as well as differences between short-period and broadband stacks suggest that the weak arrivals originate by reflection from laterally varying structure in the mantle near the subduction zone. The only structure consistently producing near-source and near-receiver reflections is the "410 km" discontinuity, which varies in depth by ±10 km, and has an impedance contrast comparable with that predicted by reference Earth models.

Introduction

Upper-mantle seismic discontinuity structure provides key information on mantle mineralogy and the configuration of mantle convection. For decades, seismic reflections and conversions have been used to infer depth and impedance contrast ('strength') of mantle discontinuities using a variety of modeling techniques [e.g., *Whitcomb and Anderson*, 1970; *Ward*, 1978; *Faber and Müller*, 1980; *Shearer*, 1990; *Revenaugh and Jordan*, 1991; *Vidale and Benz*, 1992]. In recent years seismic stacking analyses, involving summation of large numbers of seismic waveforms, have received much attention due to the availability of digital seismic waveform data from regional arrays. Images of mantle discontinuity structure in distinct geographic regions have been generated using short-period arrays with hundreds of stations, yielding models of the sharpness, strength, and local depth variations of the global "660 km" and "410 km" discontinuities [e.g., *Vidale and Benz*, 1992; *Wicks and Richards*, 1993; *Niu and Kawakatsu*, 1995]. Stacking analyses also suggested the intermittent presence of other discontinuities [e.g., *Vidale and Benz*, 1992; *Kawakatsu and Niu*, 1994; *Zhang*, 1994].

A major challenge in interpreting short-period waveform stacks is the variability observed between events, and the presence of many arrivals that are not interpretable with simple layered structures. To assess the robustness of short-period stacks for identification of mantle layering we compare stacks of short-period signals with stacks of broadband data for four recent deep (h > 550 km) earthquakes in South America (Figure 1a). The short-period data were recorded by stations of the Northern California Seismic Network (NCSN) and the Southern California Seismic Network (SCSN). The number of useful traces for each event exceeds 100, and the stations span the length of California. The broadband data were recorded by the 20+ stations of the combined TERRAscope and Berkeley Digital Seismic Network (BDSN) (Figure 1b). California is one of the few regions in the world where direct comparison of dense arrays of short-period and broadband signals is possible. The position of the South America source region relative to California provides a favorable recording aperture that spans 10°. This results in an optimal slowness resolution in the waveform stacks.

Copyright 1995 by the American Geophysical Union.

Paper number 95GL03318
0094-8534/95/95GL-03318$03.00

Slant-stacking of short-period and broadband waveforms

Reflections and conversions of seismic waves from abrupt changes in upper mantle properties (i.e., mantle discontinuities) are generally too weak to be observed on individual traces. By summing large numbers of recordings, incoherent noise is diminished while coherent signals from mantle discontinuity interactions are enhanced. Slant-stacking involves the following steps: (1) the recordings are aligned on a reference phase (P in this study) and normalized so that the reference phase has unit amplitude. (2) for a given slowness, s_k, relative to the reference phase slowness, the *ith* trace is shifted in time by $\Delta t_i = s_k(x_i - x_{med})$, where x_i is the epicentral distance of station i, and x_{med} is the median epicentral distance of all stations. The shifted traces are summed to produce stacks for a range of slownesses from -1 s/° to 1 s/°. The slant-stack should reveal any under-side mantle reflections (p_xP and s_xP) and top-side conversions (S_xP) from mantle discontinuities at depth x near the source, as well as any coherent receiver-side reverberations (Pp_xp) which arrive between the direct P and surface reflected pP phases. The various ray geometries are illustrated in Figure 1c.

Deep earthquakes (Table 1) were chosen to maximize the separation between P and pP waves. Sources with depths of 550 to 600 km have about a 2-minute time window for observing any mantle discontinuity interaction phases. Prior to stacking, the short-period data were bandpass filtered between 2-4 s; the longest periods with sufficient signal to noise ratio. The broadband velocity waveform data were lowpass filtered to retain periods longer than 8 s, resulting in waveforms free of complexities from the rupture process.

The top graph for each event in Figure 2 displays the predicted arrival times and slownesses (relative to the P phase) of the seismic phases P, pP, sP, PcP and interaction phases for reference discontinuities at 210 km, 410 km, and 660 km depth, computed for the IASP91 reference model [*Kennett & Engdahl*, 1991]. Discontinuity reflections are characterized by arrival times and slownesses that are intermediate to those

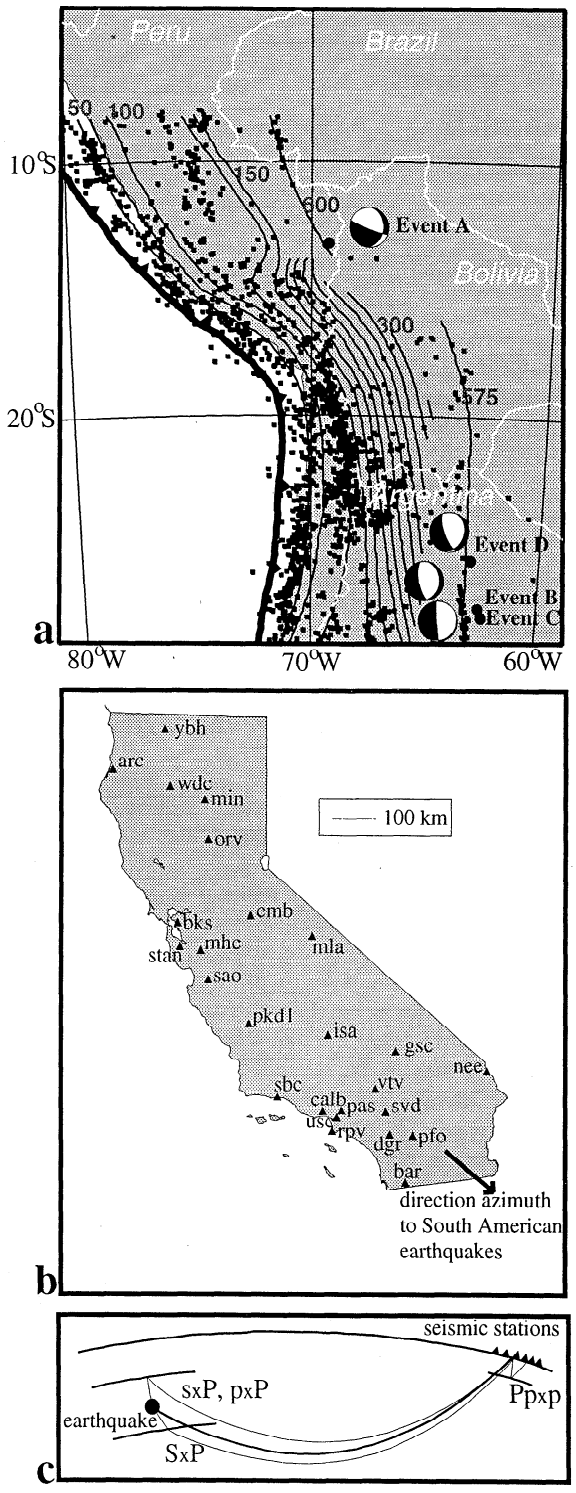

Figure 1. a. Epicenters and USGS body wave moment tensor focal mechanisms of earthquakes utilized. b. Location of broadband instruments (triangles) in California. c. Ray geometry of discontinuity interaction phases analyzed in this study.

of P and pP, while top-side conversions below the source have negative slownesses. The difference in slowness of source-side and receiver-side reflected signals that arrive close in time does not exceed 0.2 s/°, thus precise slowness resolution is required to distinguish among them for a single event. Even with short-period data one must rely on systematic variations of arrival times and slownesses in stacks determined for events with different depths. One can also seek consistency in the amplitudes of both p_xP and s_xP reflections from a given structure, but this requires use of sources with different focal mechanisms.

The contour plot for each event shows short-period stack envelopes, plotted at the same scale as the top graphs. The amplitude scale is logarithmic and truncates so that only signals greater than 1% of the maximum amplitude are visible, with colder colors indicating larger amplitudes. Resolution of arrival time and slowness are limited by the finite source duration and array aperture, respectively. The smearing of the P wave image indicates the limited resolution. Due to the large source depths, the smearing precludes identification of S660P.

The top trace of the waveform set for each event in Figure 2 is the observed broadband stack at a slowness of 0.3 s/°. This stack is representative of the entire slowness range (-1 s/°, 1 s/°) given the small travel time variations across the array with respect to the 8 s dominant period. Although lacking in slowness resolution, the broadband stack provides robust polarity and amplitude constraints on the discontinuity interaction signals. Synthetic broadband stacks, computed by a reflectivity method for one-dimensional mantle models that have only a Moho and a single discontinuity at a particular depth in the mantle, are plotted below the observations. The USGS body-wave moment tensor solutions, reported in the PDE catalogs were used. The reflection type and impedance contrast at the mantle discontinuity are specified on the left of each synthetic. Discontinuities at several upper-mantle depths were introduced to match the timing and amplitude of signals in the data, though the interpretations are not unique.

Data analysis

Some of the stronger unidentified signals observed in the short-period stacks arrive with slownesses smaller than that of the P wave. If due to horizontal discontinuities, these signals can only be attributed to S-to-P conversions at depths larger than 1000 km. However, the event-to-event variability in these small amplitude signals apparent in Figure 2, as well as in additional stacks from other earthquakes in South America not presented in this paper, suggests the presence of laterally varying velocity structure near the subduction zone. The $p_{410}P$ reflection is the only signal observed consistently in the short-period stacks. Slight time and slowness deviations from predictions for the IASP91 structure, may suggest slight topography of this discontinuity. A signal with arrival time close to $p_{210}P$ is present in the stacks of events A, B, and D, however its negative slowness and the absence of this feature for event C argues against a horizontal, "210 km" discontinuity in the source region. Scattering from a dipping reflector, possibly the subducting slab, is an alternative explanation for this signal, but it is difficult to quantify the origin of such arrivals.

Table 1. Earthquake parameters.

Event	Date	Lat (°S)	Lon (°W)	Depth (km)	M_w
A	940110	13.34	69.45	596	6.9
B	940429	28.30	63.25	562	6.9
C	940510	28.50	63.10	601	6.9
D	940819	26.64	63.42	564	6.4

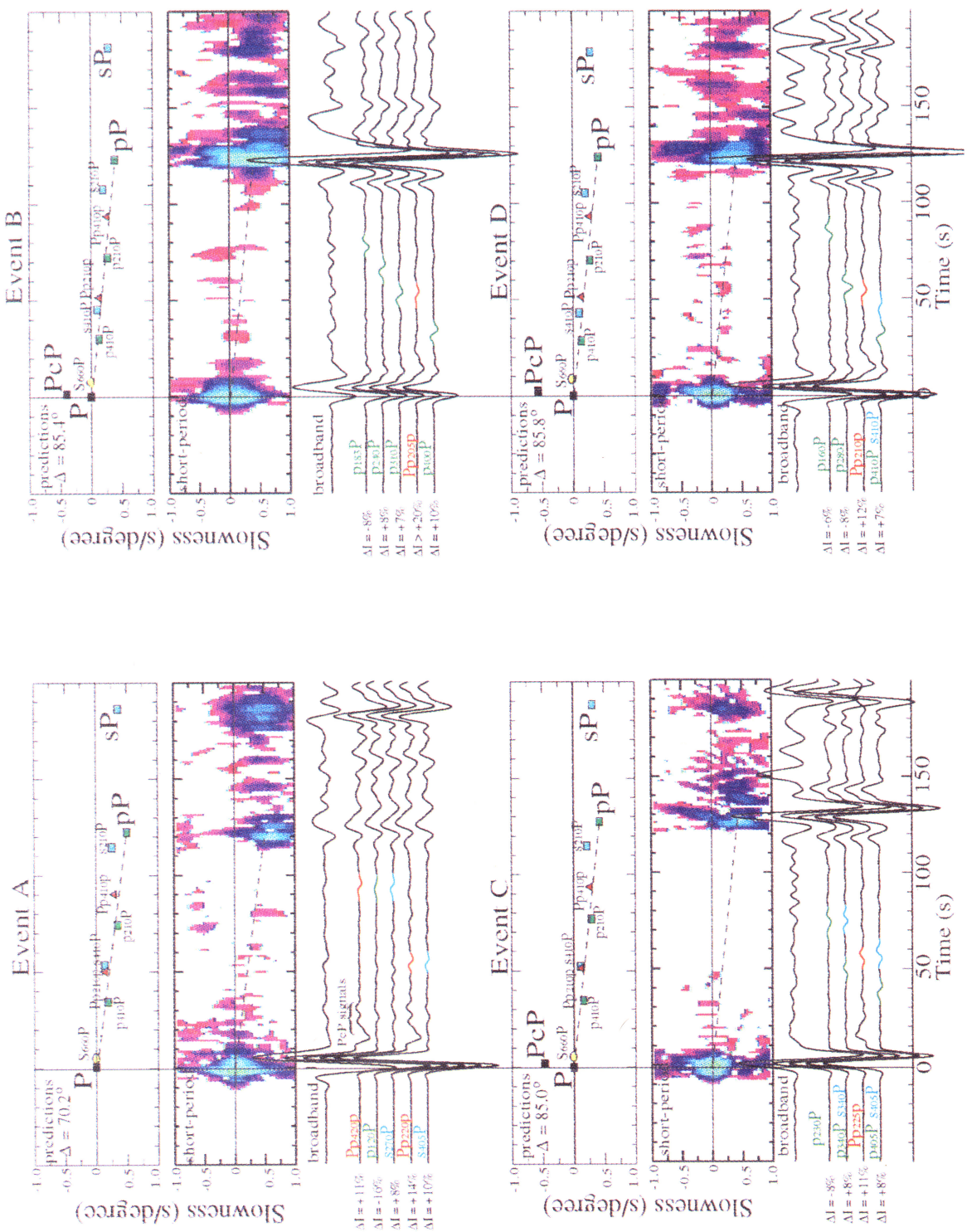

Figure 2. Slant-stack results for the four deep earthquakes. For each earthquake, the top graph provides relative arrival time and slowness of the major seismic phases (P, pP, sP, PcP) and discontinuity interaction phases from mantle discontinuities at 210 km, 410 km, and 660 km depth, based on the IASP91 [*Kennett and Engdahl*, 1991] velocity model. The contour plots are the short-period slant-stacks, at the same scale as the top graph. The top trace of the set of waveforms is the observed broadband stack, for a slowness of +0.3 s/° (relative to P). Slant-stacks of synthetics are shown below the data, for models with a Moho and a single mantle discontinuity at the depth indicated by the highlighted phase type on the left. The impedance contrasts for the associated boundary is indicated by Δ*I*.

The broadband data stacks indicate a predominance of p_xP and s_xP reflections over receiver-side reverberations. The stack for Event A, which has weak pP and sP waves, is relatively featureless, whereas the greater signal level in the stacks of Events B, C, and D is accompanied by large pP and/or sP waves. The differences in focal mechanism should be considered when trying to identify discontinuity interaction phases. Event B should show mainly p_xP arrivals, while Events C and D should show both p_xP and s_xP. Event A should preferentially exhibit receiver-side reverberations, but any s_xP should be stronger than p_xP.

Differences in the short-period and broadband stacks may reflect frequency dependence of the reflections or topography in the reflector, which is averaged differently by the different wavelengths. Receiver-side mantle reverberations undergo significant attenuation and scattering in the heterogeneous mantle under the receivers in California and are weak in high-frequency stacks [J. Revenaugh, pers. communication]. However, receiver-side crustal reverberations may still be observable in the stacks of rather heavily filtered short-period data, arriving within 10-20 s after the P wave.

Synthetics computed for various upper-mantle discontinuity models show that impedance contrasts of about 6-10% explain the amplitudes of most signals in the broadband stacks. Source-side reflections $p_{405}P$ and/or $s_{405}P$ are observed in each of the broadband stacks, suggesting a slight elevation of the 410-km discontinuity. The average P wave impedance contrast estimated for this structure is 9%, comparable with the IASP91 model (8%). The various synthetics that are shown are not meant to imply a suite of discontinuities in the mantle, but rather serve as reference for assessing polarity and timing of arrivals. Events B, C, and D have several oscillations extending from 50 s after the P wave to the pP arrival. These are consistent with under-side reflections at depths shallower than about 300 km, with the strongest arrivals just ahead of pP being under-side reflections from the Moho. From the inconsistency of these arrivals we infer that heterogeneous slab and wedge structure, rather than horizontal layering is responsible for scattering the long-period signals from this depth range.

Only for event A, for which source-side reflections are relatively small, can receiver-side reverberations, and in particular the $Pp_{420}p$ arrival, be identified. From SS precursors, *Shearer* [1993] found evidence for a 210 km discontinuity under California, and for all of our events there is some energy arriving at the corresponding time. However, identification of $Pp_{210}p$ is hampered in the stacks of Events A and C because it overlaps $s_{410}P$. For Event B and D, which have shallower source depths than Events A and C, $Pp_{210}p$ arrive approximately 10 s later than $s_{410}P$. Arrivals are present at the correct time, but modeling the feature for Event B as a receiver-side reverberation implies a very strong impedance contrast. Smaller contrasts are required to explain these arrivals with near-source reflections, but a consistent reflector is not resolved.

Discussion and Conclusions

For four deep earthquakes in South America, we have shown that stacks of short-period waveforms from closely located earthquakes are quite variable, and compare poorly with stacks of broadband recordings. This demonstrates the difficulty of deriving reliable mantle discontinuity structure from a small number of slant-stacks, even for near-by earthquakes. In addition, significant amplitude (up to 10% of the P wave amplitude) signals are observed at slownesses which cannot be explained by horizontal discontinuity structures. Although S-to-P conversions from the mid-mantle (depths larger than 1000 km) may explain some of these signals, we argue that complex structure in the slab region above the earthquakes probably contributes scattered arrivals. The only reflection consistently observed in both the short-period and broadband stacks is from a near-source discontinuity at a depth of 405 km. Forward modeling of $p_{405}P$ and $s_{405}P$ signals in broadband stacks yields an impedance contrast of about 9%, close to the value in the IASP91 model.

It is clear that short-period arrays will continue to have the advantage of larger numbers of stations and better slowness resolution, enabling identification of weak arrivals. However, broadband stacks determined for M_w = 6.4-6.9 earthquakes using 20+ waveforms can resolve reflections from structures in the mantle. Broadband data provide robust polarity and amplitude measurements, and enable forward modeling to estimate reflector depth and impedance contrast, which is difficult with short-period data. Additional work is underway to compare short-period and broadband stacks using deep earthquakes from other subduction zone regions, as well as to model shear-wave reflections and conversions in transverse and radial component broadband seismograms.

Acknowledgments. Data were provided by the seismic network operators of Caltech (TERRAscope), U.C. Berkeley (BDSN), and the USGS. We thank E. Garnero and J. Revenaugh for helpful comments on the manuscript. Constructive reviews were provided by D. Helmberger, H. Kawakatsu, P. Shearer, and an anonymous reviewer. This research was supported by the U.S. Geological Survey (USGS) Department of the Interior, under USGS award number 1434-94-G2442. Institute of Tectonics contribution number 273.

References

Faber, S., and G. Müller, *Sp* phases from the transition zone between upper and lower mantle, *Bull. Seismol. Soc. Am.*, *70*, 487-508, 1980.

Kawakatsu, H., and F. Niu, Seismic evidence for a 920 km discontinuity in the mantle, *Nature*, *371*, 301-305, 1994.

Kennett, B. L. N., and E. R. Engdahl, Travel times for global earthquake location and phase identification, *Geophys. J. Int.*, *105*, 429-465, 1991.

Niu, F., and H. Kawakatsu, Direct evidence for the undulation of the 660-km discontinuity beneath Tonga: Comparison of Japan and California array data, *Geophys. Res. Lett.*, *22*, 531-534, 1995.

Revenaugh, J. S., and T. H. Jordan, Mantle layering from ScS reverberations, 3, The upper mantle, *J. Geophys. Res.*, *96*, 19,781-19,811, 1991.

Shearer, P. M., Seismic imaging of upper-mantle structure with new evidence for a 520 km discontinuity, *Nature*, *344*, 121-126, 1990.

Shearer, P. M., Global mapping of upper-mantle reflectors from long-period SS precursors, *Geophys. J. Int.*, *115*, 878-904, 1993.

Vidale, J. E., and H. M. Benz, Upper-mantle seismic discontinuities and the thermal structure of subduction zones, *Nature*, *356*, 678-683, 1992.

Ward, S. N., Long-period reflected and converted upper-mantle phases, *Bull. Seismol. Soc. Am.*, *68*, 133-153, 1978.

Whitcomb, J., and D. L. Anderson, Reflection of *P'P'* seismic waves from discontinuities in the mantle, *J. Geophys. Res.*, *75*, 5713-5728, 1970.

Wicks, C. W., and M. A. Richards, A detailed map of the 660 kilometer discontinuity beneath the Izu-Bonin subduction zone, *Science*, *261*, 1424-1427,1993.

Zhang, Z., Seismic investigation of the Earth's structure, Ph. D. Thesis, 307 pp., University of California, Santa Cruz, 1994.

M. Hagerty, T. Lay, and J. Ritsema, Institute of Tectonics, University of California, Santa Cruz, CA 95064 (e-mail: jeroen@rupture.ucsc.edu).

(Received April 27, 1995; revised August 21, 1995;
accepted October 4, 1995)